

# Multilevel iterative solvers for the edge finite element solution of the 3D Maxwell equation\*

O. V. Nechaev<sup>†</sup>      E.P. Shurina<sup>†</sup>      M.A. Botchev<sup>‡</sup>

October 26, 2006

This paper ([www.math.utwente.nl/~botchevma/efem\\_mg.pdf](http://www.math.utwente.nl/~botchevma/efem_mg.pdf)) is to appear in "Computers and Mathematics with Applications", 2007.

## Abstract

In the edge vector finite element solution of the frequency domain Maxwell equations, the presence of a large kernel of the discrete rotor operator is known to ruin convergence of standard iterative solvers. We extend the approach of [1] and, using domain decomposition ideas, construct a multilevel iterative solver where the projection with respect to the kernel is combined with the use of a hierarchical representation of the vector finite elements.

The new iterative scheme appears to be an efficient solver for the edge finite element solution of the frequency domain Maxwell equations. The solver can be seen as a variable preconditioner and, thus, accelerated by Krylov subspace techniques (e.g. GCR or FGMRES). We demonstrate the efficiency of our approach on a test problem with strong jumps in the conductivity.

**Key words:** Nédélec vector finite elements; kernel of the rotor operator; multilevel iterative solvers; hierarchical preconditioners; domain decomposition.

**AMS Subject Classification:** 65N22, 65N30, 65N55.

## 1 Introduction

When modeling electromagnetic phenomena, the so-called frequency domain approach is often used, meaning that the electromagnetic field is assumed to depend harmonically on time. This is usually justified by the nature of the field sources [2, 3]. In many modern realistic applications the electromagnetic fields have to be modeled in inhomogeneous media consisting of different materials, i.e. in media with jumps in physical properties such as conductivity and dielectric permittivity. Moreover, this often has to be done for a wide frequency range. The complexity of the models requires development and implementation of special computational schemes which satisfy certain (normal or tangential) continuity conditions of vector electric and magnetic fields across the material interfaces [2, 3, 4]. Applied to the Maxwell equations, the frequency domain approach is often combined with the reduction to a second-order partial

---

\*This work was supported by the Netherlands organization for scientific research NWO and Russian Foundation for Basic Research RFBR within Scientific cooperation programme between the Netherlands and the Russian Federation, project 047.016.003.

<sup>†</sup>Novosibirsk State Technical University, 20 K. Marx Ave., Novosibirsk 630092, Russia, [shurina@online.sinor.ru](mailto:shurina@online.sinor.ru), [howl@ngs.ru](mailto:howl@ngs.ru).

<sup>‡</sup>Corresponding author, Department of Applied Mathematics, University of Twente, P.O. Box 217, 7500 AE Enschede, The Netherlands, [m.a.botchev@math.utwente.nl](mailto:m.a.botchev@math.utwente.nl), fax: +31 53 489 4833.

differential equation of the Helmholtz type with respect to the vector complex-valued electric or magnetic field.

Nédélec [5, 6] designed two families of finite elements for the Maxwell equations where a specially chosen basis of vector functions provides the proper type of continuity of the electric or magnetic field across the boundary between the elements. These continuity properties are preserved if the material properties (such as conductivity and permittivity) differ from element to element. A comprehensive study of different variational formulations for electromagnetic problems and their discrete analogs is done in [7] where the main mathematical tools used are differential forms, De Rham complex and Helmholtz decomposition.

Spectral properties of the matrix resulting from the vector finite element discretization of this equation are characterized by the presence of a large kernel of the discrete rotor operator [1, 8]. Due to large dimension of the kernel, application of standard preconditioners usually does not give a reduction in the number of iterations or even may lead to divergence of the iterative process [1, 9, 10].

One way to tackle this problem is proposed in [1, 11], where a number of multigrid and multilevel solvers are developed. The idea is to decompose the space where the solution is searched for into the kernel and its orthogonal complement [1]. Thus, the high frequency modes of the solution and the components of the solution belonging to the kernel can be handled separately by a suitable smoothing procedure. This approach makes efficient multigrid solution of the discretized Maxwell equations possible. Based on the theoretical framework of [12] and the concepts of [1], the authors of [13] further explore the potential of multigrid methods for vector finite element solution of the frequency domain double rotor Maxwell equations. However, in [13] only the case of zero conductivity is considered. This is an easy test case (see the results presented in Section 9) though the matrix of the resulting linear system is then still indefinite.

We note that similar problems arise in numerical solution of the scalar Helmholtz equation (see e.g. [14, 15]).

The algorithms presented in this paper are based on the concepts of [1] and aim to extend them in a natural way. We develop a two-level iterative solver with a kernel projection procedure and a multiplicative iterative solver. The latter solver is based on the domain decomposition ideas and uses a hierarchical representation of the first order Nédélec elements of the second type. When applied in combination with the two-level solver it is shown to be a very efficient tool for higher order vector finite element solution of the frequency domain Maxwell equations in three-dimensional inhomogeneous media. This is confirmed by numerical experiments presented in this paper.

The structure of the paper is as follows. In Section 2 the Maxwell equations are posed. The vector variational formulation is discussed in Section 3, and in Section 4 the vector finite elements are presented. In Section 5 we construct a hierarchical representation of finite element bases and we formulate the discretized problem in Section 6. The two-level and multiplicative iterative solvers are presented in Sections 7 and 8. Numerical experiments are described in Section 9 whereafter the conclusions are drawn.

## 2 Mathematical model

The behavior of a time-harmonic electromagnetic field is described by the following system of the Maxwell equations:

$$\operatorname{rot} \mathbf{E} + i\omega \mathbf{B} = 0, \quad (1)$$

$$\operatorname{rot} \mathbf{H} - i\omega \mathbf{D} - \mathbf{J} = \mathbf{J}_0, \quad (2)$$

$$\operatorname{div} \mathbf{D} = \rho, \quad (3)$$

$$\operatorname{div} \mathbf{B} = 0, \quad (4)$$

$$\operatorname{div} \mathbf{J} + i\omega \rho = 0, \quad (5)$$

where  $\mathbf{E}$  is the intensity of the electric field,  $\mathbf{D}$  is the electric induction,  $\mathbf{H}$  is the intensity of the magnetic field,  $\mathbf{B}$  is the magnetic induction,  $\mathbf{J}$  is the current density,  $\mathbf{J}_0$  is the given source current density,  $\rho$  is the density of electric charges,  $\omega$  is the cyclic frequency,  $\varepsilon$  is the dielectric permittivity,  $\mu$  is magnetic permeability,  $\sigma$  is the electric conductivity and  $i$  is the imaginary unit. Here,  $\mathbf{E}$ ,  $\mathbf{B}$ ,  $\mathbf{D}$  and  $\mathbf{H}$  are three-dimensional vector fields defined in a domain  $\Omega \subset \mathbb{R}^3$ , and  $\varepsilon$ ,  $\mu$  and  $\sigma$  are, in general, three-dimensional positive semidefinite tensors. The constitutive relations and Ohm's law read:

$$\mathbf{D} = \varepsilon \mathbf{E}, \quad (6)$$

$$\mathbf{B} = \mu \mathbf{H}, \quad (7)$$

$$\mathbf{J} = \sigma \mathbf{E}. \quad (8)$$

We assume that the following consistency condition holds for the Maxwell equations:

$$\operatorname{div} \mathbf{J}_0 = 0. \quad (9)$$

Taking into account (3), (6), and (8), we can rewrite conservation law (5) as

$$\operatorname{div}((\sigma + i\omega\varepsilon)\mathbf{E}) = 0. \quad (10)$$

Furthermore, using (6)–(8), we reduce the system of equations (1) and (2) to a second order equation in the complex-valued vector field  $\mathbf{E}$ :

$$\operatorname{rot}(\mu^{-1}\operatorname{rot} \mathbf{E}) + k^2 \mathbf{E} = -i\omega \mathbf{J}_0, \quad k^2 = i\omega\sigma - \omega^2\varepsilon. \quad (11)$$

On the interface  $\Gamma$  between different materials the following continuity conditions hold:

$$[\mathbf{n} \times \mathbf{E}]|_{\Gamma} = 0, \quad [\mathbf{n} \cdot (\sigma + i\omega\varepsilon)\mathbf{E}]|_{\Gamma} = 0,$$

where  $\mathbf{n}$  is a normal vector with respect to the surface  $\Gamma$ .

In this paper we consider the case where the conductivity  $\sigma$  and the permittivity  $\varepsilon$  are discontinuous scalar functions on  $\Omega$  and the permeability  $\mu$  is constant. We assume that the domain  $\Omega$  is bounded and has a perfectly conducting Lipschitz-continuous boundary  $\partial\Omega$ , namely,

$$\mathbf{n} \times \mathbf{E}|_{\partial\Omega} = 0, \quad (12)$$

where  $\mathbf{n}$  is the unit outwards normal vector to  $\partial\Omega$ . Without loss of generality, we assume for simplicity that  $\Omega$  is a polyhedral domain, i.e. it can be represented as a union of tetrahedra.

### 3 Vector variational formulation

Introduce the following spaces [5, 6]

$$\begin{aligned} \mathbf{H}(\text{rot}; \Omega) &= \{ \mathbf{v} \in [\mathbf{L}^2(\Omega)]^3 : \text{rot } \mathbf{v} \in [\mathbf{L}^2(\Omega)]^3 \}, \\ \mathbf{H}_0(\text{rot}; \Omega) &= \{ \mathbf{v} \in \mathbf{H}(\text{rot}; \Omega) : \mathbf{v} \times \mathbf{n} = 0 \}, \end{aligned}$$

equipped with the norm

$$\| \mathbf{u} \|_{\text{rot}, \Omega}^2 = \int_{\Omega} \mathbf{u} \cdot \mathbf{u} \, d\Omega + \int_{\Omega} (\text{rot } \mathbf{u}) \cdot (\text{rot } \mathbf{u}) \, d\Omega$$

and inner product

$$(\mathbf{u}, \mathbf{v}) = \int_{\Omega} \mathbf{u} \cdot \mathbf{v} \, d\Omega.$$

Here and throughout the rest of the paper, functional spaces are introduced over the complex numbers. For system (11),(12), we consider the following variational formulation [1]:

**Problem 1** Find  $\mathbf{E} \in \mathbf{H}_0(\text{rot}; \Omega)$  such that for all  $\mathbf{v} \in \mathbf{H}_0(\text{rot}; \Omega)$

$$(\text{rot } (\mu^{-1} \text{rot } \mathbf{E}), \mathbf{v}) + (k^2 \mathbf{E}, \mathbf{v}) = -(i\omega \mathbf{J}_0, \mathbf{v}). \quad (13)$$

With the help of a Green formula, the first term in (13) can be rewritten as

$$\int_{\Omega} \text{rot } (\mu^{-1} \text{rot } \mathbf{E}) \cdot \mathbf{v} \, d\Omega = \int_{\Omega} (\mu^{-1} \text{rot } \mathbf{E}) \cdot (\text{rot } \mathbf{v}) \, d\Omega - \int_{\partial\Omega} \mu^{-1} [(\mathbf{v} \times \text{rot } \mathbf{E}) \cdot \mathbf{n}] \, dS,$$

where, due to the properties of the introduced spaces, the last term in the right-hand side equals zero. This yields the following vector variational formulation:

Find  $\mathbf{E} \in \mathbf{H}_0(\text{rot}; \Omega)$  such that for all  $\mathbf{v} \in \mathbf{H}_0(\text{rot}; \Omega)$

$$(\mu^{-1} \text{rot } \mathbf{E}, \text{rot } \mathbf{v}) + (k^2 \mathbf{E}, \mathbf{v}) = -(i\omega \mathbf{J}_0, \mathbf{v}). \quad (14)$$

Let the following embedding property hold

$$\text{grad } \phi \in \mathbf{H}(\text{rot}; \Omega), \quad \text{for all } \phi \in \mathbf{H}^1(\Omega), \quad (15)$$

where  $\mathbf{H}^1(\Omega)$  is the Sobolev space. Since variational problem (14) holds for all  $\mathbf{v} \in \mathbf{H}(\text{rot}; \Omega)$ , according to (15), we can take  $\mathbf{v} = \text{grad } \phi$ ,  $\phi \in \mathbf{H}^1(\Omega)$ . Then (14) takes the form

$$(\mu^{-1} \text{rot } \mathbf{E}, \text{rot } \text{grad } \phi) + (k^2 \mathbf{E}, \text{grad } \phi) = -(i\omega \mathbf{J}_0, \text{grad } \phi), \quad \text{for all } \phi \in \mathbf{H}^1(\Omega).$$

Taking into account (9) and the property  $\text{rot } \text{grad } \phi \equiv 0$ , we obtain

$$((\omega^2 \varepsilon + i\omega \sigma) \mathbf{E}, \text{grad } \phi) = 0, \quad \text{for all } \phi \in \mathbf{H}^1(\Omega), \quad (16)$$

$$\begin{aligned} ((\omega^2 \varepsilon + i\omega \sigma) \mathbf{E}, \text{grad } \phi) &= \int_{\Omega} (\omega^2 \varepsilon + i\omega \sigma) \mathbf{E} \cdot \text{grad } \phi \, d\Omega \\ &= \int_{\Omega} \text{div } [(\omega^2 \varepsilon + i\omega \sigma) \mathbf{E}] \phi \, d\Omega. \end{aligned} \quad (17)$$

It follows from (17) that (16) is a variational analog of conservation law (10). In other words, the solution of variational problem (14) satisfies conservation law (5) in a weak sense.

## 4 Nédélec elements of the first and second type

Let a partition  $T$  of the domain  $\Omega$  into a number of nonintersecting elements  $K$  be given:

$$\Omega = \bigcup_{K \in T} K, \quad K_i \cap K_j = \emptyset \quad \text{for all } K_i, K_j \in T, i \neq j.$$

Assume that  $T$  is built in such a way that the physical properties of the medium (determined by the parameters  $\varepsilon$ ,  $\mu$ , and  $\sigma$ ) are constant within each element  $K$ . Let  $h_K$  be the diameter of the element  $K$ . Define the characteristic size of the partition  $T$  as

$$h = \max_{K \in T} h_K.$$

To build discrete analogs of the variational formulations posed in Section 3, we need to introduce finite-dimensional subspaces of the space  $\mathbf{H}(\text{rot}; \Omega)$  and define interpolation functions to approximate  $\mathbf{E}$ . In this paper, Nédélec spaces of vector elements are taken as such finite-dimensional subspaces [5, 6]. These subspaces are conforming in  $\mathbf{H}(\text{rot}; \Omega)$ .

To define a finite element, one needs to specify (see e.g. [3, 5]): (i) a domain of the finite element  $K$ , (ii) a space  $P(K)$  of polynomials on  $K$ , (iii) a space  $\mathcal{A}$  of degrees of freedom which are linear functionals on  $P(K)$ .

For vector finite elements on  $\mathbb{R}^3$  the polynomial space  $P$  is a subspace of  $C^\infty(\bar{K})^3$ . For each  $\mathbf{u} \in C^\infty(\bar{K})^3$  there exists a unique interpolant  $\Pi \mathbf{u} \in P$  such that

$$\alpha_i(\mathbf{u} - \Pi \mathbf{u}) = 0, \quad \forall \alpha_i \in \mathcal{A}.$$

In [5] the following result is proved:

**Lemma 1** *Finite element  $(K, \mathcal{A}, P)$  is conforming in  $\mathbf{H}(\text{rot}; \Omega)$  if and only if*

- (i) *for any two adjacent elements  $K_1$  and  $K_2$  with a common face  $f$ , tangential components of interpolants  $\Pi_1 \mathbf{u}$  and  $\Pi_2 \mathbf{u}$  (defined on  $K_1$  and  $K_2$ , respectively) coincide on the face  $f$ , or, equivalently,*
- (ii) *for any degree of freedom  $\alpha_i$  defined on the face  $f$ , it holds: if  $\alpha_i(p) = 0$ ,  $p \in P$  then  $(\mathbf{n} \times p)|_f = 0$ , where  $\mathbf{n}$  is the normal vector on  $f$ .*

In other words, vector finite elements that are conforming in  $\mathbf{H}(\text{rot}; \Omega)$  should guarantee tangential continuity of the field across the inter-element interfaces. There are no restrictions on the normal components of the field which effectively means that the normal components can be discontinuous. When modeling the electric field  $\mathbf{E}$ , this is a key property of the vector finite elements.

Define first type Nédélec vector finite elements of the  $k$ th degree for tetrahedral and hexahedral elements [5]. Let  $K$  be a tetrahedron. The space  $\mathcal{A}$  of degrees of freedom consists of

- (a)  $\int_e (\mathbf{u} \cdot \mathbf{t}) q ds, \forall q \in P_{k-1}(K),$
- (b)  $\int_f \mathbf{u} \times \mathbf{n} \cdot \mathbf{q} d\gamma, \forall \mathbf{q} \in (P_{k-2}(K))^2,$
- (c)  $\int_K \mathbf{u} \cdot \mathbf{q} dx, \forall \mathbf{q} \in (P_{k-3}(K))^3,$

where  $P_k(K)$  is the space of polynomials on  $K$  of degree not greater than  $k$  and  $\mathbf{t}$  is the unit tangential vector along edge  $e$ . Nédélec proved [5] that the number of degrees of freedom defined in (a) is  $6k$ , in (b) is  $4k(k-1)$  and in (c) is  $\frac{1}{2}k(k-1)(k-2)$ . This means that the degrees of freedom of a first-type element are defined on the element edges for  $k=1$ , on the element edges and faces for  $k=2$  and on the element edges, faces and inside the element for  $k \geq 3$ .

In [6], Nédélec extended the definition of the degrees of freedom in a vector finite element by introducing vector finite elements of the second type. The degrees of freedom of such an element on a tetrahedron are defined as

$$(a) \int_e (\mathbf{u} \cdot \mathbf{t}) q ds, \forall q \in P_k,$$

$$(b) \int_f \mathbf{u} \cdot \mathbf{q} d\gamma, \forall \mathbf{q} \in G_{k-1}(f),$$

$$(c) \int_K \mathbf{u} \cdot \mathbf{q} dx, \forall \mathbf{q} \in G_{k-2}(K),$$

where  $G_k = (P_{k-1})^3 \oplus \hat{P}_{k-1} \cdot r$ , with  $\hat{P}_k$  being the space of the polynomials of degree  $k$ ,  $r = (x, y, z)^T$ . Here, the number of degrees of freedom defined by expression (a) for the edges is  $6(k+1)$ , by expression (b) for the faces is  $4(k-1)(k+1)$ , defined by expression (c) inside the tetrahedra is  $\frac{1}{2}(k-2)(k-1)(k+1)$ . The interpolation error of the vector Nédélec elements of the second type is  $O(h^{k+1})$  [6].

It follows from the definition of Nédélec elements of the first and second type that a first order element of the first type is a zero order element of the second type. Note that zero and first order elements of the second type have only degrees of freedom associated with the edges. For  $k=0$ , instead of the definition given above, the degrees of freedom can be defined by prescribing a value of the tangential component of the field in any arbitrary point of the associated edge. For  $k=1$ , this can be done by prescribing values in two points. This means also that the first order elements of the first type approximate the field tangential component by constant values, whereas the first order elements of the second type by linear functions.

In this paper, first order Nédélec vector finite elements of the first and second type are used.

## 5 Hierarchy of the vector basis functions

For a vector function  $\mathbf{u}(x, y, z,)$  its interpolant  $\mathbf{u}^h$  is defined on a tetrahedral element  $K$  as

$$\mathbf{u}^h(x, y, z) = \sum_{i \in S} \alpha_i(\mathbf{u}) \mathbf{w}_i^h(x, y, z), \quad (18)$$

where  $\alpha_i$  are the degrees of freedom,  $S$  is the index set of the degrees of freedom,  $\mathbf{w}_i^h$  are the basis functions, and  $(x, y, z)$  is a point in  $\mathbb{R}^3$ .

Let  $p_i = (x_i, y_i, z_i)$ ,  $i = 1, 2, 3, 4$  be the coordinates of an arbitrary tetrahedron  $K$  in the partition  $T$  (see Figure 1) and  $\lambda_i(x, y, z)$ ,  $i = 1, 2, 3, 4$  the three-dimensional barycentric coordinates of the point  $(x, y, z) \in K$  with respect to the tetrahedron vertices. Then the local first order vector basis functions  $\mathbf{w}_j^K$  of the first type are defined as

$$\mathbf{w}_j^K = \lambda_{i_1} \nabla \lambda_{i_2} - \lambda_{i_2} \nabla \lambda_{i_1}, \quad j = 1, \dots, 6, \quad (19)$$

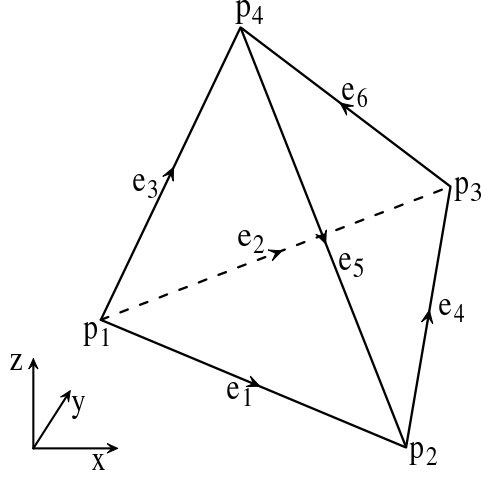


Figure 1: Local numeration of vertices and edges in a tetrahedral finite element.

where the edge  $j$  points from the vertex  $i_1$  to the vertex  $i_2$ . The correspondence between the local edge numbers  $j$  and the local vertex numbers  $i_1, i_2$  is shown in Figure 1. For  $\mathbf{w}_j^K$  it holds

$$\mathbf{t}_j \cdot \mathbf{w}_j^K = \frac{1}{l_j}, \quad (20)$$

where  $\mathbf{t}_j$  and  $l_j$  are respectively the unit tangential vector and the length of the edge  $j$ . Define the degrees of freedom as (cf. (18)):

$$\alpha_j(\mathbf{u}) = (\mathbf{u}(x_j^c, y_j^c, z_j^c) \cdot \mathbf{t}_j) l_j, \quad j = 1, \dots, 6, \quad (21)$$

where  $(x_j^c, y_j^c, z_j^c)$  are the coordinates of the center point of edge  $j$ . Besides (21), there are other ways to define  $\alpha_j(\mathbf{u})$ , for example,

$$\alpha_j(\mathbf{u}) = \frac{l_j}{2} (\mathbf{u}(x_{i_1}, y_{i_1}, z_{i_1}) + \mathbf{u}(x_{i_2}, y_{i_2}, z_{i_2})) \cdot \mathbf{t}_j, \quad j = 1, \dots, 6. \quad (22)$$

The first way of computing  $\alpha_j(\mathbf{u})$  (cf. (21)) is cheaper, since it requires one evaluation of  $\mathbf{u}(x, y, z)$  per edge. However, as will be shown later, choice (22) has advantages with respect to constructing the hierarchical basis.

The global basis function  $\mathbf{w}_{j_{\text{global}}}$  of the edge with the global number  $j_{\text{global}}$  is defined as

$$\mathbf{w}_{j_{\text{global}}}(x, y, z) = \begin{cases} \mathbf{w}_{j_{\text{local}}}^K(x, y, z), & \text{if edge } j_{\text{global}} \in K, \\ 0, & \text{if edge } j_{\text{global}} \notin K, \end{cases} \quad (23)$$

where  $K$  is the element of the partition  $T$  such that  $(x, y, z) \in K$  and  $j_{\text{local}}$  is the local number of the edge  $j_{\text{global}}$  in the element  $K$ .

We will denote spaces of the first order basis functions of the first type by  $H^h(\text{rot}; \Omega; 1)$ .

Weak form (16) of the charge conservation law remains to hold true after discretization due to some embedding properties of the discrete finite element spaces. Indeed, consider  $H^h(\text{rot}; \Omega; 1)$  and introduce a discrete subspace  $H^h(\text{grad}; \Omega; 1)$  of local basis functions taken to be barycentric coordinate functions  $\lambda_i$ ,  $i = 1, 2, 3, 4$ :

$$\phi_i^K = \lambda_i, \quad i = 1, 2, 3, 4. \quad (24)$$

It is easy to check that

$$\begin{aligned}\nabla\phi_1^K &= \nabla\lambda_1 = -\mathbf{w}_1^K - \mathbf{w}_2^K - \mathbf{w}_3^K, \\ \nabla\phi_2^K &= \nabla\lambda_2 = \mathbf{w}_1^K - \mathbf{w}_4^K + \mathbf{w}_5^K, \\ \nabla\phi_3^K &= \nabla\lambda_3 = \mathbf{w}_2^K + \mathbf{w}_4^K - \mathbf{w}_6^K, \\ \nabla\phi_4^K &= \nabla\lambda_4 = \mathbf{w}_3^K - \mathbf{w}_5^K + \mathbf{w}_6^K,\end{aligned}$$

in other words, gradients of the functions from  $\mathbb{H}^h(\text{grad}; \Omega; 1)$  belong to  $\mathbb{H}^h(\text{rot}; \Omega; 1)$ :

$$u \in \mathbb{H}^h(\text{grad}; \Omega; 1) \quad \Rightarrow \quad \nabla u \in \mathbb{H}^h(\text{rot}; \Omega; 1). \quad (25)$$

We now introduce a space  $\mathbb{H}^h(\text{rot}; \Omega; 2)$  of local first order vector basis functions of the second type:

$$\mathbf{w}_{j,1}^K = \lambda_{i_1} \nabla \lambda_{i_2}, \quad \mathbf{w}_{j,2}^K = \lambda_{i_2} \nabla \lambda_{i_1}, \quad j = 1, \dots, 6, \quad (26)$$

where the edge  $j$  points from the vertex  $i_1$  to the vertex  $i_2$  and, for each edge  $j$ , two local basis functions  $\mathbf{w}_{j,1}^K$  and  $\mathbf{w}_{j,2}^K$  are defined. For correspondence between the local edge and vertex numbers see Figure 1. Relations similar to (20) can be obtained:

$$\mathbf{t}_1 \cdot \mathbf{w}_{1,1}^K = \frac{1}{l_1} \lambda_1, \quad \dots, \quad \mathbf{t}_6 \cdot \mathbf{w}_{6,2}^K = \frac{1}{l_6} \lambda_4,$$

where  $\mathbf{t}_j$  is the unit tangent vector along edge  $j$ . For functions from  $\mathbb{H}^h(\text{rot}; \Omega; 2)$ , introduce degrees of freedom in (18) as

$$\begin{aligned}\alpha_{j,1}(\mathbf{u}) &= (\mathbf{u}(x_{i_1}, y_{i_1}, z_{i_1}) \cdot \mathbf{t}_j) l_j, \\ \alpha_{j,2}(\mathbf{u}) &= (\mathbf{u}(x_{i_2}, y_{i_2}, z_{i_2}) \cdot \mathbf{t}_j) l_j, \quad j = 1, \dots, 6,\end{aligned}$$

so that two degrees of freedom are associated with each edge  $j$ . Global functions of the subspace  $\mathbb{H}^h(\text{rot}; \Omega; 2)$  are defined similarly to (23).

A discrete subspace  $\mathbb{H}^h(\text{grad}; \Omega; 2)$  corresponding to  $\mathbb{H}^h(\text{rot}; \Omega; 2)$  consists of scalar second order local basis functions

$$\begin{aligned}\phi_1^K &= \lambda_1(2\lambda_1 - 1), & \phi_2^K &= \lambda_2(2\lambda_2 - 1), \\ \phi_3^K &= \lambda_3(2\lambda_3 - 1), & \phi_4^K &= \lambda_4(2\lambda_4 - 1), \\ \phi_5^K &= 4\lambda_1\lambda_2, & \phi_6^K &= 4\lambda_1\lambda_3, \\ \phi_7^K &= 4\lambda_1\lambda_4, & \phi_8^K &= 4\lambda_2\lambda_3, \\ \phi_9^K &= 4\lambda_2\lambda_4, & \phi_{10}^K &= 4\lambda_3\lambda_4.\end{aligned}$$

Let a discrete space  $M$  of finite elements be a direct sum of spaces  $V$  and  $W$ :

$$M = V \oplus W.$$

We will call a basis of  $M$  hierarchical if it is a union of bases of the spaces  $V$  and  $W$  [16].

To build a hierarchical basis of  $\mathbb{H}^h(\text{rot}; \Omega; 2)$ , we represent  $\mathbb{H}^h(\text{rot}; \Omega; 2)$  as

$$\mathbb{H}^h(\text{rot}; \Omega; 2) = \mathbb{H}^h(\text{rot}; \Omega; 1) \oplus W,$$

where the space  $W$  remains to be defined. It follows from (19) and (26) that  $W$  should be a space spanned by the functions

$$\begin{aligned} \mathbf{w}_1^K &= \lambda_1 \nabla \lambda_2 + \lambda_2 \nabla \lambda_1, & \mathbf{w}_2^K &= \lambda_1 \nabla \lambda_3 + \lambda_3 \nabla \lambda_1, \\ \mathbf{w}_3^K &= \lambda_1 \nabla \lambda_4 + \lambda_4 \nabla \lambda_1, & \mathbf{w}_4^K &= \lambda_2 \nabla \lambda_3 + \lambda_3 \nabla \lambda_2, \\ \mathbf{w}_5^K &= \lambda_4 \nabla \lambda_2 + \lambda_2 \nabla \lambda_4, & \mathbf{w}_6^K &= \lambda_3 \nabla \lambda_4 + \lambda_4 \nabla \lambda_3. \end{aligned}$$

This yields the following hierarchical basis for  $H^h(\text{rot}; \Omega; 2)$ :

$$\begin{aligned} \mathbf{w}_{1,1}^K &= \lambda_1 \nabla \lambda_2 - \lambda_2 \nabla \lambda_1, & \mathbf{w}_{2,1}^K &= \lambda_1 \nabla \lambda_3 - \lambda_3 \nabla \lambda_1, \\ \mathbf{w}_{3,1}^K &= \lambda_1 \nabla \lambda_4 - \lambda_4 \nabla \lambda_1, & \mathbf{w}_{4,1}^K &= \lambda_2 \nabla \lambda_3 - \lambda_3 \nabla \lambda_2, \\ \mathbf{w}_{5,1}^K &= \lambda_4 \nabla \lambda_2 - \lambda_2 \nabla \lambda_4, & \mathbf{w}_{6,1}^K &= \lambda_3 \nabla \lambda_4 - \lambda_4 \nabla \lambda_3, \\ \mathbf{w}_{1,2}^K &= \lambda_1 \nabla \lambda_2 + \lambda_2 \nabla \lambda_1, & \mathbf{w}_{2,2}^K &= \lambda_1 \nabla \lambda_3 + \lambda_3 \nabla \lambda_1, \\ \mathbf{w}_{3,2}^K &= \lambda_1 \nabla \lambda_4 + \lambda_4 \nabla \lambda_1, & \mathbf{w}_{4,2}^K &= \lambda_2 \nabla \lambda_3 + \lambda_3 \nabla \lambda_2, \\ \mathbf{w}_{5,2}^K &= \lambda_4 \nabla \lambda_2 + \lambda_2 \nabla \lambda_4, & \mathbf{w}_{6,2}^K &= \lambda_3 \nabla \lambda_4 + \lambda_4 \nabla \lambda_3. \end{aligned} \tag{27}$$

The degrees of freedom for the basis functions  $\mathbf{w}_{j,1}^K$ ,  $j = 1, \dots, 6$ , are defined according to (22) and for the basis functions  $\mathbf{w}_{j,2}^K$  as

$$\alpha_{j,2}(\mathbf{u}) = \frac{b_j}{2} (\mathbf{u}(x_{i_2}, y_{i_2}, z_{i_2}) - \mathbf{u}(x_{i_1}, y_{i_1}, z_{i_1})) \cdot \mathbf{t}_j, \quad j = 1, \dots, 6.$$

We can now build a hierarchical basis for the space  $H^h(\text{grad}; \Omega; 2)$ . Since embedding property (25) holds for  $H^h(\text{grad}; \Omega; 1)$  and  $H^h(\text{rot}; \Omega; 1)$ , we take  $H^h(\text{grad}; \Omega; 1)$  as the first direct summand for  $H^h(\text{grad}; \Omega; 2)$ . Then, the local basis functions of the second direct summand are

$$\begin{aligned} \phi_1^K &= \lambda_1 \lambda_2, & \phi_2^K &= \lambda_1 \lambda_3, \\ \phi_3^K &= \lambda_1 \lambda_4, & \phi_4^K &= \lambda_2 \lambda_3, \\ \phi_5^K &= \lambda_2 \lambda_4, & \phi_6^K &= \lambda_3 \lambda_4. \end{aligned} \tag{28}$$

Combining basis functions (24) and (28), we obtain the following hierarchical basis for  $H^h(\text{grad}; \Omega; 2)$ :

$$\begin{aligned} \phi_1^K &= \lambda_1, & \phi_2^K &= \lambda_2, \\ \phi_3^K &= \lambda_3, & \phi_4^K &= \lambda_4, \\ \phi_5^K &= \lambda_1 \lambda_2, & \phi_6^K &= \lambda_1 \lambda_3, \\ \phi_7^K &= \lambda_1 \lambda_4, & \phi_8^K &= \lambda_2 \lambda_3, \\ \phi_9^K &= \lambda_2 \lambda_4, & \phi_{10}^K &= \lambda_3 \lambda_4. \end{aligned} \tag{29}$$

It is not difficult to see that gradients of the scalar basis functions of  $H^h(\text{grad}; \Omega; 2)$  are linear

combinations of the basis functions of  $H^h(\text{rot}; \Omega; 2)$ . Indeed,

$$\begin{aligned}
\nabla\phi_1^K &= \nabla\lambda_1 = -\mathbf{w}_{1,1}^K - \mathbf{w}_{2,1}^K - \mathbf{w}_{3,1}^K, \\
\nabla\phi_2^K &= \nabla\lambda_2 = \mathbf{w}_{1,1}^K - \mathbf{w}_{4,1}^K + \mathbf{w}_{5,1}^K, \\
\nabla\phi_3^K &= \nabla\lambda_3 = \mathbf{w}_{2,1}^K + \mathbf{w}_{4,1}^K - \mathbf{w}_{6,1}^K, \\
\nabla\phi_4^K &= \nabla\lambda_4 = \mathbf{w}_{3,1}^K - \mathbf{w}_{5,1}^K + \mathbf{w}_{6,1}^K, \\
\nabla\phi_5^K &= \nabla(\lambda_1\lambda_2) = \mathbf{w}_{1,2}^K, \\
\nabla\phi_6^K &= \nabla(\lambda_1\lambda_3) = \mathbf{w}_{2,2}^K, \\
\nabla\phi_7^K &= \nabla(\lambda_1\lambda_4) = \mathbf{w}_{3,2}^K, \\
\nabla\phi_8^K &= \nabla(\lambda_2\lambda_3) = \mathbf{w}_{4,2}^K, \\
\nabla\phi_9^K &= \nabla(\lambda_2\lambda_4) = \mathbf{w}_{5,2}^K, \\
\nabla\phi_{10}^K &= \nabla(\lambda_3\lambda_4) = \mathbf{w}_{6,2}^K.
\end{aligned}$$

We thus proved that

$$u \in H^h(\text{grad}; \Omega; 2) \quad \Rightarrow \quad \nabla u \in H^h(\text{rot}; \Omega; 2). \quad (30)$$

In the remainder of the paper the hierarchical bases of  $H^h(\text{rot}; \Omega; 2)$  and  $H^h(\text{grad}; \Omega; 2)$  on tetrahedral meshes are used.

## 6 Discrete variational formulations

To build a discrete analog of the variational problem, we approximate the elements from  $H(\text{rot}; \Omega)$  by the elements from the discrete subspace  $H^h(\text{rot}; \Omega)$ . Consider the following discrete analog of variational Problem 1:

**Discrete variational problem 1** *For given  $\mathbf{J}_{0,\text{re}} \in H(\text{rot}; \Omega)$  find  $\mathbf{E}_{\text{re}}^h \in H_0^h(\text{rot}; \Omega)$  and  $\mathbf{E}_{\text{im}}^h \in H_0^h(\text{rot}; \Omega)$  such that for all  $\mathbf{v}_1^h \in H_0^h(\text{rot}; \Omega)$  and  $\mathbf{v}_2^h \in H_0^h(\text{rot}; \Omega)$*

$$\begin{aligned}
(\mu^{-1}\text{rot } \mathbf{E}_{\text{re}}^h, \text{rot } \mathbf{v}_1^h) - (\omega^2\varepsilon \mathbf{E}_{\text{re}}^h, \mathbf{v}_1^h) - (\omega\sigma \mathbf{E}_{\text{im}}^h, \mathbf{v}_1^h) &= 0, \\
(\mu^{-1}\text{rot } \mathbf{E}_{\text{im}}^h, \text{rot } \mathbf{v}_2^h) - (\omega^2\varepsilon \mathbf{E}_{\text{im}}^h, \mathbf{v}_2^h) + (\omega\sigma \mathbf{E}_{\text{re}}^h, \mathbf{v}_2^h) &= (\omega \mathbf{J}_{0,\text{re}}, \mathbf{v}_2^h).
\end{aligned}$$

Since embedding properties (25),(30) hold for the built discrete subspaces  $H^h(\text{grad}; \Omega)$  and  $H^h(\text{rot}; \Omega)$ , the approximate solution  $\mathbf{E}^h = \mathbf{E}_{\text{re}}^h + i\mathbf{E}_{\text{im}}^h$  satisfies the following weak form of the charge conservation law (cf. (10),(16))

$$\begin{aligned}
(-\omega\varepsilon \mathbf{E}_{\text{im}}^h - \sigma \mathbf{E}_{\text{re}}^h, \nabla u_1^h) &= 0 \quad \text{for all } u_1^h \in H_0^h(\text{grad}; \Omega), \\
(\omega\varepsilon \mathbf{E}_{\text{re}}^h - \sigma \mathbf{E}_{\text{im}}^h, \nabla u_2^h) &= 0 \quad \text{for all } u_2^h \in H_0^h(\text{grad}; \Omega).
\end{aligned}$$

Expanding the real and imaginary components of the unknown field  $\mathbf{E}^h$  into the basis functions of  $H_0^h(\text{rot}; \Omega)$  and choosing the test functions  $\mathbf{v}_1^h$  and  $\mathbf{v}_2^h$  as the same basis functions, we arrive at the following linear system

$$Ax = b, \quad A = \begin{bmatrix} D+B & -C \\ C & D+B \end{bmatrix}, \quad x = \begin{bmatrix} e_{\text{re}} \\ e_{\text{im}} \end{bmatrix}, \quad b = \begin{bmatrix} 0 \\ f \end{bmatrix}, \quad (31)$$

where  $e_{\text{re}}$  and  $e_{\text{im}}$  are the vectors containing the basis expansion coefficients of  $\mathbf{E}_{\text{re}}^h$  and  $\mathbf{E}_{\text{im}}^h$ , respectively, and the entries of the matrices  $D$ ,  $B$  and  $C$  and the vector  $f$  read

$$\begin{aligned} [D]_{i,j} &= (\mu^{-1} \text{rot } \mathbf{w}_i^h, \text{rot } \mathbf{w}_j^h), & [B]_{i,j} &= -(\varepsilon \omega^2 \mathbf{w}_i^h, \mathbf{w}_j^h), \\ [C]_{i,j} &= (\sigma \omega \mathbf{w}_i^h, \mathbf{w}_j^h), & [f]_i &= (\omega \mathbf{J}_{0,\text{re}}, \mathbf{w}_i^h). \end{aligned}$$

We apply the following preconditioner

$$\tilde{A}x = \tilde{b}, \quad \tilde{A} = P^{-1}A, \quad \tilde{b} = P^{-1}b, \quad P = \begin{bmatrix} \text{Diag}(D+B) & -\text{Diag}(C) \\ \text{Diag}(C) & \text{Diag}(D+B) \end{bmatrix}, \quad (32)$$

where  $\text{Diag}(\cdot)$  denotes the diagonal part of a matrix. In the sequel of the paper we assume that this preconditioner is always applied first, before any action is taken.

## 7 Two-level iterative solver

### 7.1 Description of the two-level solver

Let system (32) be  $n \times n$ . For simplicity of notation, we omit the tilde sign in (32):

$$Ax = b. \quad (32')$$

Let  $V$  be an  $m$ -dimensional subspace of  $\mathbb{R}^n$ ,  $m \leq n$  and  $x_0 \in \mathbb{R}^n$  an initial guess vector. Consider the Galerkin orthogonal correction to the approximate solution  $x_0$  by an element of  $V$ :

*For a given initial guess vector  $x_0$ , find  $z \in V$  such that the residual vector of the new approximate solution  $x_1 = x_0 + z$  is orthogonal to  $V$ :*

$$(b - Ax_1, v) = 0, \quad \text{for all } v \in V. \quad (33)$$

If  $P$  is an  $n \times m$  matrix whose columns span  $V$ , then (33) can be rewritten as

$$P^T(b - Ax_1) = 0, \quad (34)$$

where  $x_1 = x_0 + z$ ,  $z = Py \in V$  for a certain vector  $y \in \mathbb{R}^m$ . Since

$$\begin{aligned} P^T(b - Ax_1) &= P^T(b - A(x_0 + Py)) = P^T(b - Ax_0 - APy) = \\ &= P^T(b - Ax_0) - P^T APy = 0, \end{aligned}$$

we have

$$y = (P^T AP)^{-1} P^T r_0, \quad (35)$$

where  $r_0 = b - Ax_0$  is the initial residual vector. Note that the matrix  $P^T AP$  is nonsingular because  $P$  is assumed to be of full rank. Introducing the error vectors  $\epsilon_0 = x - x_0$  and  $\epsilon_1 = x - x_1$  and noticing that  $r_0 = A\epsilon_0$ , we obtain

$$\begin{aligned} \epsilon_1 &= x - x_1 = x - x_0 - P(P^T AP)^{-1} P^T r_0 \\ &= \epsilon_0 - P(P^T AP)^{-1} P^T A\epsilon_0 = (I - P(P^T AP)^{-1} P^T A)\epsilon_0, \end{aligned} \quad (36)$$

where  $I$  is the identity matrix. In a similar way we get the following relation for the residual vectors:

$$r_1 = (I - AP(P^T AP)^{-1} P^T) r_0. \quad (37)$$

```

Two-level algorithm  $S_V(A, b, x_0, \nu)$ 
 $r_0 = b - Ax_0,$ 
for  $i = 1, 2, \dots$ 
     $g = P^T r_{i-1},$ 
     $y \approx (P^T AP)^{-1}g$  (call  $y = S(P^T AP, g, \gamma_P)$ ),
     $x_{i-1/2} = x_{i-1} + Py,$ 
     $r_{i-1/2} = b - Ax_{i-1/2},$ 
     $z \approx A^{-1}r_{i-1/2}$  (call  $z = S(A, r_{i-1/2}, \gamma)$ ),
     $x_i = x_{i-1/2} + z,$ 
     $r_i = b - Ax_i,$ 
    if  $\|r_i\| < \nu\|b\|$  then stop, return  $x_i,$ 
end for

```

Figure 2: An algorithmic description of the two-level iterative solver.

Assume that in the correction step the system with the matrix  $P^T AP$  is solved approximately, so that instead of  $(P^T AP)^{-1}P^T r_0$  we have

$$(P^T AP)^{-1}P^T r_0 + \delta,$$

where  $\delta$  is an error vector. Replacing in (36), (37) the term  $(P^T AP)^{-1}P^T r_0$  by  $(P^T AP)^{-1}P^T r_0 + \delta$ , we obtain

$$\begin{aligned} \epsilon_1 &= (I - P(P^T AP)^{-1}P^T A)\epsilon_0 + P\delta, \\ r_1 &= (I - AP(P^T AP)^{-1}P^T)r_0 + AP\delta. \end{aligned} \tag{38}$$

Note that if the vector  $(P^T AP)^{-1}P^T r_0$  is computed approximately by solving the linear system  $(P^T AP)u = P^T r_0$  inexactly with an iterative method, then the residual vector  $p = P^T r_0 - (P^T AP)u$  is related to  $\delta$  as  $\delta = -(P^T AP)^{-1}p$ . In other words, although  $\delta$  is not readily available, it can be made arbitrarily small in norm by controlling the norm of the residual  $p$ .

Denote by  $S(A, b, \gamma)$  an iterative solver which, for a given matrix  $A$ , vector  $b$  and scalar  $\gamma > 0$ , delivers an approximate solution  $\tilde{x}$  to the linear system  $Ax = b$  such that

$$\|b - A\tilde{x}\| < \gamma\|b\|.$$

We assume, by definition of  $S(A, b, \gamma)$ , that the initial guess vector in the solver  $S(A, b, \gamma)$  is always taken zero. Based on the considered inexact Galerkin orthogonal correction procedure, we can formulate a two-level iterative solver presented in Figure 2.

If the inner iterative solver  $z = S(A, r_{i-1/2}, \gamma)$  in this algorithm converges then

$$\|r_i\| < \gamma\|r_{i-1/2}\| = \gamma \frac{\|r_{i-1/2}\|}{\|r_{i-1}\|} \|r_{i-1}\|$$

and, for convergence of the algorithm, it is sufficient to require that

$$\gamma \frac{\|r_{i-1/2}\|}{\|r_{i-1}\|} < 1 \quad \Leftrightarrow \quad \gamma < \frac{\|r_{i-1}\|}{\|r_{i-1/2}\|}.$$

Thus, algorithm  $S_V(A, b, x_0, \nu)$  converges if, at each iteration  $i$ ,  $\gamma$  is chosen as

$$\gamma = \alpha \frac{\|r_{i-1}\|}{\|r_{i-1/2}\|},$$

with  $\alpha$  being a chosen scalar,  $0 < \alpha < 1$ . Note that, with this choice of  $\gamma$ , computational work in the algorithm  $S_V(A, b, x_0, \nu)$  varies with the iteration number because the inner iterative solvers may require a different number of iterations for convergence.

Other, simpler ways of choosing  $\gamma_P$  and  $\gamma$  can work in practice. In all experiments presented in this paper we simply take fixed values  $\gamma_P = 0.1$  and  $\gamma = 0.9$ . The values are chosen experimentally and work well for a wide range of test problems. Indeed, it appears to be important for convergence to solve the projected system with the matrix  $P^T A P$  relatively accurately. However, the main computational costs in the two-level solver are connected with the step  $z \approx A^{-1} r_{i-1/2}$ , even though the value  $\gamma = 0.9$  gives a mild stopping criterion.

We note that convergence of inexact or the so-called inner-outer iterative schemes has been extensively studied [17, 18, 19], especially in connection with a proper choice of stopping criteria in the inner solvers. Incorporating one of the approaches proposed in the literature may further tune the performance of the two-level solver. This is, however, left beyond the scope of this paper.

## 7.2 Choice of the subspace $V$

Consider now the application of the two-level iterative solver to linear system (32'). Since the matrix  $A$  of linear system (31) is nonsymmetric, we use the stabilized biconjugate gradient iterative BiCGSTAB [20, 21, 22] as the inner iterative solvers  $S(P^T A P, g, \gamma_P)$  and  $S(A, r_{i-1/2}, \gamma)$  in the two-level solver (cf. Figure 2).

It is sensible to choose the subspace  $V$  as the kernel space  $N^h(\text{rot}; \Omega)$  of the rotor operator in the space  $H^h(\text{rot}; \Omega)$ :

$$N^h(\text{rot}; \Omega) = \left\{ \mathbf{u} \in H^h(\text{rot}; \Omega) : \text{rot } \mathbf{u} = 0 \right\}.$$

Due to the embedding property (cf. (25),(30)) and the fact that  $\text{rot grad} \equiv 0$ , we have

$$H^h(\text{grad}; \Omega) = N^h(\text{rot}; \Omega).$$

With this choice of  $V$ , the columns of the matrix  $P$  (recall that  $\text{span} P = V$ ) are the coordinates of the gradients of the basis functions of  $H_0^h(\text{grad}; \Omega)$  with respect to the basis of  $H_0^h(\text{rot}; \Omega)$ . This means that the linear system

$$P^T A P u = P^T r \tag{39}$$

is equivalent to the following variational problem:

*For given  $\mathbf{F}_{0,\text{re}}, \mathbf{F}_{0,\text{im}} \in H(\text{rot}; \Omega)$  find  $U_{\text{re}}^h \in H_0^h(\text{grad}; \Omega)$  and  $U_{\text{im}}^h \in H_0^h(\text{grad}; \Omega)$  such that for all  $v_1^h \in H_0^h(\text{grad}; \Omega)$  and  $v_2^h \in H_0^h(\text{grad}; \Omega)$*

$$\begin{aligned} (\mu^{-1} \text{rot grad } U_{\text{re}}^h, \text{rot grad } v_1^h) - (\omega^2 \varepsilon \text{grad } U_{\text{re}}^h, \text{grad } v_1^h) - (\omega \sigma \text{grad } U_{\text{im}}^h, \text{grad } v_1^h) &= (\mathbf{F}_{0,\text{im}}, \text{grad } v_2^h), \\ (\mu^{-1} \text{rot grad } U_{\text{im}}^h, \text{rot grad } v_2^h) - (\omega^2 \varepsilon \text{grad } U_{\text{im}}^h, \text{grad } v_2^h) + (\omega \sigma \text{grad } U_{\text{re}}^h, \text{grad } v_2^h) &= (\mathbf{F}_{0,\text{re}}, \text{grad } v_2^h), \end{aligned}$$

which, due to the property  $\text{rot grad} \equiv 0$ , can be simplified to

$$\begin{aligned} -(\omega^2 \varepsilon \text{grad} U_{\text{re}}^h, \text{grad} v_1^h) - (\omega \sigma \text{grad} U_{\text{im}}^h, \text{grad} v_1^h) &= (\mathbf{F}_{0,\text{im}}, \text{grad} v_2^h), \\ -(\omega^2 \varepsilon \text{grad} U_{\text{im}}^h, \text{grad} v_2^h) + (\omega \sigma \text{grad} U_{\text{re}}^h, \text{grad} v_2^h) &= (\mathbf{F}_{0,\text{re}}, \text{grad} v_2^h). \end{aligned}$$

We note that the matrix of projected linear system (39) can be obtained by the finite element technique rather than by direct matrix multiplications, which are expensive.

The two-level iterative solver with this choice of the subspace  $V$  will be denoted by  $S_{N^h(\text{rot};\Omega)}(A, b, x_0, \nu)$ .

## 8 Multiplicative iterative solver

### 8.1 Description of the solver

Let  $V_1, V_2 \in \mathbb{R}^n$  be subspaces such that

$$V_1 \cup V_2 = \mathbb{R}^n, \quad V_1 \cap V_2 \neq \emptyset$$

and let the columns of matrices  $P_1$  and  $P_2$  span the subspaces  $V_1$  and  $V_2$ , respectively. Using the Galerkin orthogonal corrections (cf. (33)–(35)) alternatively with respect to  $V_1$  and  $V_2$ , a multiplicative Schwarz solver for system (32') can be formulated as shown in Figure 3 (see e.g. [22]). Here  $S_j(P_j^T A P_j, g_j, \gamma_j)$ ,  $j = 1, 2$  are inner iterative solvers which, for a zero initial guess, deliver approximate solution to the systems  $(P_j^T A P_j)y_j = g_j$  such that the following stopping criterion is satisfied

$$\|g_j - (P_j^T A P_j)y_j\| < \gamma_j \|g_j\|, \quad j = 1, 2.$$

In this multiplicative iterative scheme, the error vector  $\epsilon_i = x - x_i$  satisfies [22]

$$\epsilon_i = (I - P_2(P_2^T A P_2)^{-1} P_2^T A)(I - P_1(P_1^T A P_1)^{-1} P_1^T A)\epsilon_{i-1},$$

so that it is sufficient for convergence to require that

$$\|(I - P_2(P_2^T A P_2)^{-1} P_2^T A)(I - P_1(P_1^T A P_1)^{-1} P_1^T A)\| < 1.$$

We now explain how the stopping parameters  $\gamma_j$  of the inner solvers can be chosen. Note that (cf. (38))

$$r_{i-1/2} = \underbrace{(I - AP_1(P_1^T A P_1)^{-1} P_1^T A)r_{i-1}}_{=r_{i-1/2}^{\text{exact}}} - AP_1(P_1^T A P_1)^{-1}p,$$

where  $p$  is the residual of the inner solver  $S_1(P_1^T A P_1, g_1, \gamma_1)$  and  $r_{i-1/2}^{\text{exact}}$  is the “exact” residual vector corresponding to the case  $p = 0$ . It is realistic to assume that  $\|AP_1(P_1^T A P_1)^{-1}p\| \approx \|p\|$ , so that

$$\|r_{i-1/2}\| \leq \|r_{i-1/2}^{\text{exact}}\| + \|p\|.$$

Due to the inner stopping criterion it holds  $\|p\| < \gamma_1 \|P_1^T r_{i-1}\|$ . Assume that the process converges for  $p = 0$ , i.e.

$$\|r_{i-1/2}^{\text{exact}}\| = \beta \|r_{i-1}\|, \quad 0 < \beta < 1.$$

Multiplicative Schwarz algorithm:

$$r_0 = b - Ax_0,$$

for  $i = 1, 2, \dots$

$$g_1 = P_1^T r_{i-1},$$

$$y_1 \approx (P_1^T A P_1)^{-1} g_1 \quad (\text{call } y_1 = S_1(P_1^T A P_1, g_1, \gamma_1)),$$

$$x_{i-1/2} = x_{i-1} + P_1 y_1,$$

$$r_{i-1/2} = b - A x_{i-1/2},$$

$$g_2 = P_2^T r_{i-1/2},$$

$$y_2 \approx (P_2^T A P_2)^{-1} g_2 \quad (\text{call } y_2 = S_2(P_2^T A P_2, g_2, \gamma_2)),$$

$$x_i = x_{i-1/2} + P_2 y_2,$$

$$r_i = b - A x_i,$$

if  $x_i$  satisfies a stopping criterion then stop, return  $x_i$ ,

end for

Figure 3: An algorithmic description of the multiplicative solver.

We want  $p$  to be comparable in norm with  $\beta \|r_{i-1}\|$ , so that  $\|r_{i-1/2}\|$  is of the same order of magnitude as  $\|r_{i-1/2}^{\text{exact}}\|$ . This can be achieved by taking  $\gamma_1 = \|r_{i-1/2}^{\text{exact}}\|/\|r_{i-1}\|$  because then

$$\begin{aligned} \|r_{i-1/2}\| &\leq \|r_{i-1/2}^{\text{exact}}\| + \|p\| \\ &< \|r_{i-1/2}^{\text{exact}}\| + \gamma_1 \|P_1^T r_{i-1}\| \\ &= \|r_{i-1/2}^{\text{exact}}\| + \|r_{i-1/2}^{\text{exact}}\|/\|r_{i-1}\| \|P_1^T r_{i-1}\| \approx 2\|r_{i-1/2}^{\text{exact}}\|. \end{aligned}$$

In practice the value of residual reduction  $\|r_{i-1/2}^{\text{exact}}\|/\|r_{i-1}\|$  is unknown beforehand and we use an approximation, namely, residual reduction achieved at the previous outer iteration  $i-1$ :

$$\gamma_1 = \begin{cases} \|r_{i-3/2}\|/\|r_{i-2}\|, & \text{if } i > 1, \\ 0.1, & \text{if } i = 1. \end{cases}$$

Analogously, we take

$$\gamma_2 = \begin{cases} \|r_{i-1}\|/\|r_{i-3/2}\|, & \text{if } i > 1, \\ 0.1, & \text{if } i = 1. \end{cases}$$

This simple strategy for choosing  $\gamma_j$  works very well in practice and is used in all numerical experiments presented in this paper.

## 8.2 Choice of the subspaces $V_1$ , $V_2$ and the inner solvers

We now define spaces

$$\begin{aligned} N^h(\text{rot}; \Omega; 1) &= \{\mathbf{u} \in H^h(\text{rot}; \Omega; 1) : \text{rot } \mathbf{u} = 0\}, \\ N^h(\text{rot}; \Omega; 2) &= \{\mathbf{u} \in H^h(\text{rot}; \Omega; 2) : \text{rot } \mathbf{u} = 0\}. \end{aligned}$$

We have shown (see (27)) that  $H^h(\text{rot}; \Omega; 2)$  is spanned by the basis functions of  $H^h(\text{rot}; \Omega; 1)$  and by gradients of scalar functions, so that

$$H^h(\text{rot}; \Omega; 2) = H^h(\text{rot}; \Omega; 1) \cup N^h(\text{rot}; \Omega; 2), \quad H^h(\text{rot}; \Omega; 1) \cap N^h(\text{rot}; \Omega; 2) = N^h(\text{rot}; \Omega; 1).$$

This motivates the following choice of the spaces  $V_1$  and  $V_2$  in the multiplicative Schwarz algorithm:

$$V_1 = H^h(\text{rot}; \Omega; 1), \quad V_2 = N^h(\text{rot}; \Omega; 2).$$

It follows from the definitions of these subspaces that the matrices  $P_1^T A P_1$  and  $P_2^T A P_2$  correspond to discrete variational problems posed for the vector Helmholtz equation in the spaces  $H^h(\text{rot}; \Omega; 1)$  and  $N^h(\text{rot}; \Omega; 2)$ , respectively. Thus, the linear systems with the matrices  $P_1^T A P_1$  and  $P_2^T A P_2$  can be computed using the finite element technique.

Depending on the matrix properties, for the inner iterative solver  $S_1(P_1^T A P_1, g_1, \gamma_1)$  either the conjugate gradient (CG) or the BiCGSTAB method was taken [21, 22, 20]. Due to the definition of the hierarchical basis of  $H^h(\text{grad}; \Omega; 2)$  (see (29)), it holds

$$N^h(\text{rot}; \Omega; 1) \subset N^h(\text{rot}; \Omega; 2).$$

Based on this observation, for the inner iterative solver  $S_2(P_2^T A P_2, g_2, \gamma_2)$  we choose the two-level solver  $S_V(P_2^T A P_2, g_2, 0, \gamma_2)$  with  $V = N^h(\text{rot}; \Omega; 1)$ .

## 9 Numerical experiments

We test the performance of the two-level and the multiplicative solvers for the following model problem: boundary value problem (11), (12) is solved in the cubic domain  $\Omega = [-0.5, 0.5]^3$ . The domain is cut by the plane  $x = 0.25$  into two subdomains, where the conductivity  $\sigma$  has values  $\sigma_1, \sigma_2$ , respectively. The dielectric permittivity is constant in the whole domain, so that  $\varepsilon = \varepsilon_1 = \varepsilon_2$  (see Figure 4). In the first subdomain a coil is placed, with an alternating electric current of 1 A and 14 MHz. For the numerical solution of this problem we follow the procedure described in Sections 3–6 and employ the iterative solvers from Sections 7 and 8.

All the computations presented in this Section were done on a PC with the Athlon-XP +1800 processor and 512 Mb memory. The computations were done on a sequence of unstructured tetrahedral meshes  $T_i$ , see Table 1. In all runs, the iterations of the solvers are stopped as soon as the outer residual norm is reduced by a factor of  $10^6$ .

Table 1: The length  $h_{\max}$  of the largest edge and dimensions of the discrete spaces for the unstructured tetrahedral meshes used in the tests. All the meshes were built with the NETGEN mesh generator (see <http://www.hpfem.jku.at/netgen/>).

	$h_{\max}$	$H^h(\text{rot}; \Omega; 1)$	$N^h(\text{rot}; \Omega; 1)$	$H^h(\text{rot}; \Omega; 2)$	$N^h(\text{rot}; \Omega; 2)$
$T_1$	$2.5 \cdot 10^{-1}$	8776	1474	17552	10250
$T_2$	$8.84 \cdot 10^{-2}$	63756	9632	127512	73388
$T_3$	$6.25 \cdot 10^{-2}$	236364	34204	472728	270568

The first point we make is that standard Krylov subspace solvers, when applied to system (32'), converge very slowly or do not converge at all (see Figures 5 and 6). The convergence deteriorates as discontinuity in  $\sigma$  becomes more pronounced.

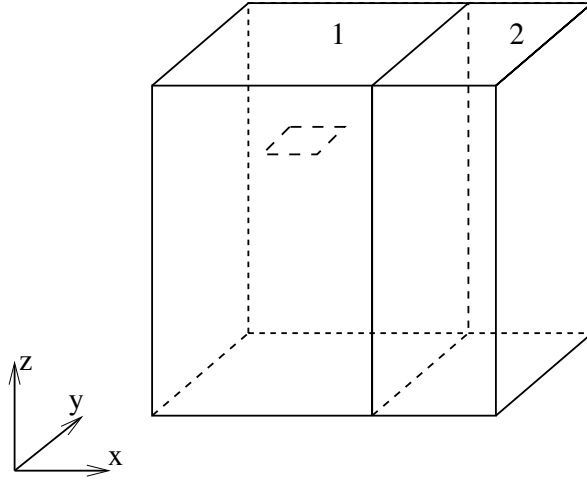


Figure 4: The domain  $\Omega$  in the model problem, divided into two subdomains, with a coil in the first subdomain.

$$\sigma_1 = \sigma_2 = 1$$

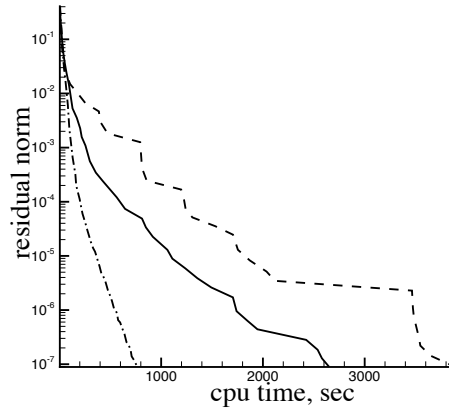


Figure 5: Convergence curves for the case  $\sigma_1 = \sigma_2 = 1$ , mesh  $T_2$  (dash-dotted: the multiplicative solver, solid: the two-level solver, dashed: BiCGSTAB).

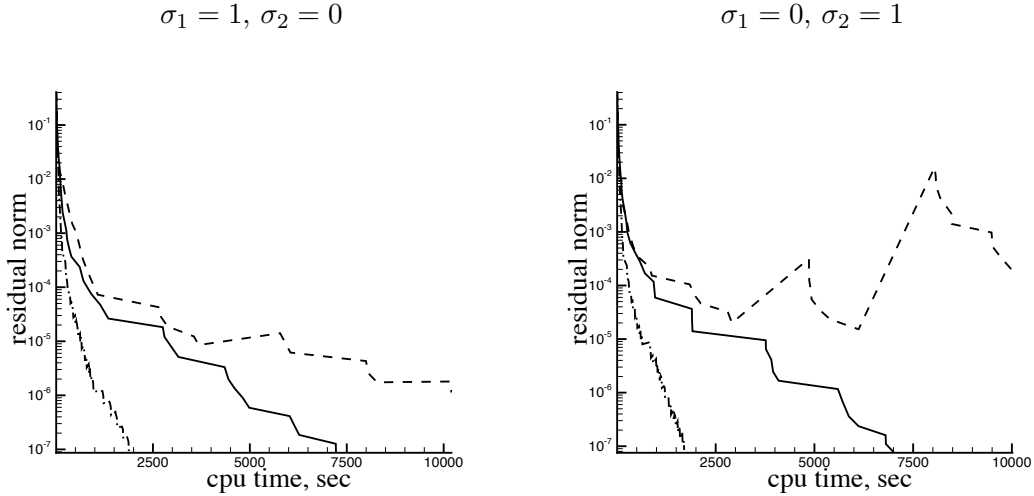


Figure 6: Convergence curves for the cases  $\sigma_1 = 1, \sigma_2 = 0$  (left) and  $\sigma_1 = 0, \sigma_2 = 1$  (right), mesh  $T_2$  (dash-dotted: the multiplicative solver, solid: the two-level solver, dashed: BiCGSTAB).

Table 2: The CPU time (sec) of the multiplicative iterative solver for different meshes and conductivity values  $\sigma_1, \sigma_2$ .

$(\sigma_1, \sigma_2)$	(1,1)	(0,0)	(1,10)	(1,0.1)	(1,0)	(10,1)	(0.1,1)	(0,1)
$T_1$	4	3	5	5	5	4	5	6
$T_2$	64	53	92	93	118	51	93	119
$T_3$	767	544	1101	1457	1879	590	1545	1702

Next, we examine the performance of the two-level and multiplicative solver for different meshes and the conductivity values  $\sigma_1, \sigma_2$  (see Tables 2 and 3). It is clear that the performance strongly depends on the conductivity values, especially when the mesh gets finer.

To gain more insight in the convergence behavior of the two-level and multiplicative solvers we list the number of iterations done by the solvers in Tables 4–6. We see that on fine meshes the work in the multiplicative solver is dominated by the inner iterations with respect to the subspace  $V_1 = H^h(\text{rot}; \Omega; 1)$  (Table 4), whereas the number of the inner iterations with respect to the kernel (Table 5) does not grow as the mesh gets finer. A similar trend is observed for the two-level solver: the work in the solver is dominated by the inner iterations with respect to the subspace  $H^h(\text{rot}; \Omega; 2)$  (we report the number of the inner iterations only with respect to this subspace, see Table 6). The convergence of both the two-level and the multiplicative solver deteriorates as the mesh gets finer, and this deterioration is more visible for the two-level solver.

In the experiments with the multiplicative solver we observed that BiCGSTAB may fail in the course of the inner iterations with respect to the subspace  $V_1 = H^h(\text{rot}; \Omega; 1)$ . This can be cured by replacing BiCGSTAB with GMRES, which is, however, expensive. It turned out that neglecting the failure in the inner iterations and going on with the outer iterations

Table 3: The CPU time (sec) of the two-level iterative solver  $S_{N^h(\text{rot};\Omega;2)}(A, b, x_0, \nu)$  for different meshes and conductivity values  $\sigma_1, \sigma_2$ .

$(\sigma_1, \sigma_2)$	(1,1)	(0,0)	(1,10)	(1,0.1)	(1,0)	(10,1)	(0.1,1)	(0,1)
$T_1$	6	3	3	8	8	5	8	10
$T_2$	122	56	118	196	215	71	205	269
$T_3$	2651	1005	1674	6957	7224	1364	5774	7022

Table 4: Total number of the inner BiCGSTAB iterations done by the multiplicative solver in the inner solver calls with respect to the subspace  $H^h(\text{rot};\Omega;1)$  (line  $y_1 = S_1(P_1^T A P_1, g_1, \gamma_1)$  in Figure 3) for different meshes and conductivity values  $\sigma_1, \sigma_2$ .

$(\sigma_1, \sigma_2)$	(1,1)	(0,0)	(1,10)	(1,0.1)	(1,0)	(10,1)	(0.1,1)	(0,1)
$T_1$	277	457	206	569	567	124	578	589
$T_2$	627	315	622	1183	1541	305	1436	1703
$T_3$	1157	376	1264	2791	2884	661	3037	4310

Table 5: Total number of the inner BiCGSTAB iterations done by the multiplicative solver in the inner solver calls with respect to the subspace  $N^h(\text{rot};\Omega;2)$  (line  $y_2 = S_2(P_2^T A P_2, g_2, \gamma_2)$  in Figure 3) for different meshes and conductivity values  $\sigma_1, \sigma_2$ .

$(\sigma_1, \sigma_2)$	(1,1)	(0,0)	(1,10)	(1,0.1)	(1,0)	(10,1)	(0.1,1)	(0,1)
$T_1$	133	56	241	206	235	245	181	177
$T_2$	132	39	157	214	219	137	163	173
$T_3$	145	38	255	198	204	98	294	260

Table 6: Total number of the inner BiCGSTAB iterations done by the two-level solver  $S_{N^h(\text{rot};\Omega;2)}(A, b, x_0, \nu)$  in the inner solver calls with respect to the subspace  $H^h(\text{rot};\Omega;2)$  (line  $z = S(A, r_{i-1/2}, \gamma)$  in Figure 2) for different meshes and conductivity values  $\sigma_1, \sigma_2$ .

$(\sigma_1, \sigma_2)$	(1,1)	(0,0)	(1,10)	(1,0.1)	(1,0)	(10,1)	(0.1,1)	(0,1)
$T_1$	217	115	156	356	376	91	356	387
$T_2$	781	165	481	823	897	201	1028	1176
$T_3$	1192	260	789	2381	2831	322	4309	2237

Table 7: The CPU time (sec) of the multiplicative iterative solver accelerated by GCR(10) for different meshes and conductivity values  $\sigma_1, \sigma_2$ .

$(\sigma_1, \sigma_2)$	(1,1)	(0,0)	(1,10)	(1,0.1)	(1,0)	(10,1)	(0.1,1)	(0,1)
$T_1$	4	3	4	4	4	4	4	4
$T_2$	54	44	61	75	157	45	77	84
$T_3$	726	500	1116	1487	1710	603	1307	1689

is better for the overall performance.

One iteration of the multiplicative solver can be seen as an action of a special variable preconditioner. This leads to an idea to combine the solver with a Krylov subspace iterative method allowing for a variable preconditioner, such as GCR or GMRES $\star$  [21, 23] or FGMRES [24].

We have tried to accelerate the multiplicative solver by combining it with the GCR method (this yields a variant of the GMRES $\star$  method [21]). It turned out that an efficient way to do this is to apply the projections with respect to the subspaces  $V_1 = \mathbb{H}^h(\text{rot}; \Omega; 1)$  and  $V_2 = \mathbb{N}^h(\text{rot}; \Omega; 2)$  alternately, so that the first projection is done at odd outer iterations while the second at even iterations. The CPU times for this preconditioned GCR(10) method are presented in Table 7. Comparing Tables 2 and 7, we see that the GCR acceleration hardly leads to an improvement in the overall performance. This suggests that the multiplicative scheme has a potential as a powerful stand-alone solver.

## 10 Conclusions

We have designed an efficient iterative solver for linear systems resulting from the edge finite element discretization of the frequency domain Maxwell equations. The key idea is to combine the projection with respect to the kernel of the rotor operator with a projection with respect to lower order finite elements. This combination can naturally be done in the framework of domain decomposition methods. The kernel projection is necessary for convergence, whereas the use of lower order elements through the hierarchical basis yields further significant reduction in the CPU time and a much faster convergence. We have also shown that the multiplicative solver can be combined with the Krylov subspace techniques which allow for a variable preconditioner (GMRES $\star$ , FGMRES).

## Acknowledgements

The authors thank anonymous referees for suggesting several improvements.

## References

- [1] R. Hiptmair. Multigrid method for Maxwell’s equations. *SIAM J. Numer. Anal.*, 36(1):204–225, 1999.

- [2] Alain Bossavit. *Computational electromagnetism. Variational formulations, complementarity, edge elements*. Electromagnetism. Academic Press Inc., San Diego, CA, 1998.
- [3] Peter Monk. *Finite Element Methods for Maxwell's Equations*. Oxford University Press, 2003.
- [4] Zhiming Chen, Qiang Du, and Jun Zou. Finite element methods with matching and nonmatching meshes for Maxwell equations with discontinuous coefficients. *SIAM J. Numer. Anal.*, 37(5):1542–1570 (electronic), 2000.
- [5] J.-C. Nédélec. Mixed finite elements in  $\mathbf{R}^3$ . *Numer. Math.*, 35(3):315–341, 1980.
- [6] J.-C. Nédélec. A new family of mixed finite elements in  $\mathbf{R}^3$ . *Numer. Math.*, 50(1):57–81, 1986.
- [7] R. Hiptmair. Finite elements in computational electromagnetism. *Acta Numer.*, 11:237–339, 2002.
- [8] H. Igarashi. On the property of the curl-curl matrix in finite element analysis with edge elements. *IEEE Transactions on Magnetics*, 37(5 (part 1)):3129–3132, 2001.
- [9] H. Igarashi and T. Honma. On convergence of iccg applied to finite-element equation for quasi-static fields. *IEEE Transactions on Magnetics*, 38(2 (part 1)):565–568, 2002.
- [10] I. Perugia. A mixed formulation for 3D magnetostatic problems: theoretical analysis and face-edge finite element approximation. *Numer. Math.*, 84(2):305–326, 1999.
- [11] Rudolf Beck and Ralf Hiptmair. Multilevel solution of the time-harmonic Maxwell's equations based on edge elements. *Internat. J. Numer. Methods Engrg.*, 45(7):901–920, 1999.
- [12] Douglas N. Arnold, Richard S. Falk, and Ragnar Winther. Multigrid in  $H(\text{div})$  and  $H(\text{curl})$ . *Numer. Math.*, 85(2):197–217, 2000.
- [13] Jayadeep Gopalakrishnan, Joseph E. Pasciak, and Leszek F. Demkowicz. Analysis of a multigrid algorithm for time harmonic Maxwell equations. *SIAM J. Numer. Anal.*, 42(1):90–108 (electronic), 2004.
- [14] Howard C. Elman, Oliver G. Ernst, and Dianne P. O'Leary. A multigrid method enhanced by Krylov subspace iteration for discrete Helmholtz equations. *SIAM J. Sci. Comput.*, 23(4):1291–1315 (electronic), 2001.
- [15] Y. A. Erlangga, C. W. Oosterlee, and C. Vuik. A novel multigrid based preconditioner for heterogeneous Helmholtz problems. *SIAM J. Sci. Comput.*, 27(4):1471–1492 (electronic), 2006.
- [16] Randolph E. Bank. Hierarchical bases and the finite element method. *Acta Numer.*, 5:1–43, 1996.
- [17] Gene H. Golub and Michael L. Overton. The convergence of inexact Chebyshev and Richardson iterative methods for solving linear systems. *Numer. Math.*, 53:571–593, 1988.

- [18] Eldar Giladi, Gene H. Golub, and Joseph B. Keller. Inner and outer iterations for the Chebyshev algorithm. *SIAM J. Numer. Anal.*, 35(1):300–319, 1998.
- [19] Zhong-Zhi Bai, Gene H. Golub, and Michael K. Ng. Hermitian and skew-Hermitian splitting methods for non-Hermitian positive definite linear systems. *SIAM J. Matrix Anal. Appl.*, 24(3):603–626, 2003.
- [20] Henk A. van der Vorst. BiCGSTAB: a fast and smoothly converging variant of BiCG for the solution of nonsymmetric linear systems. *SIAM J. Sci. Stat. Comput.*, 13(2):631–644, 1992.
- [21] Henk A. van der Vorst. *Iterative Krylov methods for large linear systems*. Cambridge University Press, 2003.
- [22] Y. Saad. Iterative methods for sparse linear systems. Book out of print, 2000. Available at URL <http://www-users.cs.umn.edu/~saad/books.html>.
- [23] Henk A. van der Vorst and Cees Vuik. GMRESR: a family of nested GMRES methods. *Numer. Lin. Alg. Appl.*, 1:369–386, 1994.
- [24] Youcef Saad. A flexible inner–outer preconditioned GMRES algorithm. *SIAM J. Sci. Comput.*, 14:461–469, 1993.